Journal of Sciences, Islamic Republic of Iran 31(1): 51 - 62 (2020) http://jsciences.ut.ac.ir
University of Tehran, ISSN 1016-1104

The Effect of Silica Coating on the Drug Release Profile and Biocompatibility of Nano-MOF-5

K. Tabatabaeian[1*], M. Simayee[1], A. Fallah Shojaie[1], F. Mashayekhi[2], M. Hadavi[2]

[1] *Department of Chemistry, Faculty of Sciences, University of Guilan, Rasht, Islamic Republic of Iran*
[2] *Department of Biology, Faculty of Sciences, University of Guilan, Rasht, Islamic Republic of Iran*

Received: 15 July 2019 / Revised: 18 September 2019 / Accepted: 28 December 2019

Abstract

The purpose of this study was the surface modification of nano MOF-5 (NMOF-5) or IRMOF-1 ($Zn_4O(C_8H_4O_4)_3$) in order to prevent its rapid degradation in the phosphate-buffered saline (PBS), along with the simultaneous increase in its biocompatibility. The NMOF-5 sample was synthesized under the ultrasound irradiation and then it was loaded with acetaminophen and ibuprofen. Each assembly (NMOF-5@drug) was then coated with a silica layer. The obtained nanoparticles were identified by FT-IR spectroscopy, N_2 adsorption porosimetry (BET), X-ray powder diffraction (XRD), the thermogravimetric analysis (TGA), and the field emission scanning electron microscopy (FE-SEM). UV/Vis spectroscopy was used to determine the release profile of the drugs from the bare and silica coated assemblies. Silica coating resulted in an enhanced stability in PBS, and the sustained release of each drug was achieved within 3 days. MTT (Methylthiazolyldiphenyl-tetrazolium bromide) assay on NIH3T3 mouse embryonic fibroblast cells as a model of the cell line showed that silica coating NMOF-5 with silica leads in the more biocompatibility and less cytotoxicity. The cell viability was increased up to 100% for the silica coated NMOF-5 compared to the bare NMOF-5. NMOF-5 and NMOF-5@silica were utilized in the injectable drug delivery for the first time. In this study, the toxicological studies about silica coated NMOF-5 in the drug delivery systems were developed.

Keywords: NMOF-5; Ibuprofen; Acetaminophen; Silica; Drug delivery.

Introduction

Polymers play an important role in the human life and they are used in a variety of applications such as separation [1], sensors [2], biomedicine [3] and catalysts [4].

Metal-organic frameworks (MOFs), also recognized as porous coordination polymers, are the self-assembled three-dimensional (3D) networks. They are constructed from various metal ions or metal-containing clusters, identified as the secondary building units (SBUs) and multidentate organic linkers (such as carboxylates,

* Corresponding author: Tel: +981333362207; Fax: +981333320066; Email: taba@guilan.ac.ir

sulfonates and tetrazolates) [5]. These crystalline porous materials have attracted special interest of the scientists for their intriguing structure, exceptionally great internal surface areas, tailorable chemistry, permanent porosity and tunable properties. Therefore, MOFs are well-studied in many applications such as the catalysis [6, 7], the separation [8], the gas storage [9], the chemical sensing [10], the light harvesting [11] and the biomedicine [12, 13].

Despite significant advances in biology and medicine, current drug therapies are associated with some limitations like the nonspecific targeting, poor physiological stability, and low cell membrane permeability [14]. So, in order to improve human health care, the targeted drug delivery systems have been studied in many scientific communities [15-17]. Generally, a sustained release of the drug over a customizable period of time is highly favorable and this can be achieved by using nano metal-organic frameworks (NMOFs) as the novel drug carriers. Their facile synthesis and biodegradable structure make them the promising platforms for the drug delivery, compared to the other nanocarriers [18].

The enhanced performance of amine functionalized with MIL-101(Cr) $\{Cr_3OH(H_2O)_2O(C_8H_4O_4)_3 \cdot nH_2O\}$ for the loading and release of ibuprofen has been shown by *Formiga et al.* [19]. The NH_2-MIL-101(Cr) $\{Cr_3OH(H_2O)_2O[(COO)C_6H_3NH_2(COO)]_3 \cdot nH_2O\}$ indicated a higher (10%) loading capacity and a lower amount of release (10%) during the same period of time (6 days), compared to MIL-101(Cr). *Wu et al.* prepared the γ-Fe_2O_3@MIL-53(Al) $\{\gamma\text{-}Fe_2O_3@Al(OH)(O_2C\text{-}C_6H_4\text{-}CO_2)\}$ via pyrolysis of Fe(acac)$_3$@MIL-53(Al) [20]. The loading percentage of ibuprofen in γ-Fe_2O_3@MIL-53(Al) was about 9.91 wt% and the release time lasted for 5 days.

However, biomedical applications of NMOFs could be affected by two key factors, namely, their stability and surface modifiability. It has been reported that coating with silica increases the blood circulation half-life of the NMOFs [18]. When MIL-101(Fe) $\{Fe_3OH(H_2O)_2O(C_8H_4O_4)_3 \cdot nH_2O\}$ was modified with amino-terephthalate ligands, followed by the incorporation of cisplatin prodrug (12.8 wt%) and the subsequent coating with a silica shell, the drug release time was increased from 14 h to 72 h [21]. Despite their promising potential for the drug delivery, NMOFs should be monitored for their possible toxic effects on the human health. In vitro experiments can be used in order to study their cytotoxicity effects on the various cell lines.

In the present study, nano MOF-5 (NMOF-5) or IRMOF-1 ($Zn_4O(C_8H_4O_4)_3$) was chosen because of its instability in water, degradability in phosphate buffer and novelty as a carrier for the injectable drugs. Ibuprofen and acetaminophen were loaded in NMOF-5 and NMOF-5@silica for the first time. Moreover, the toxicological studies about NMOF-5@silica were explored for the first time. Afterward, NMOF-5 was coated by silica to preserve them from rapid degradability. Then, the release of the drugs and the cytotoxicity of NMOFs were studied. NMOF-5@silica was introduced as an efficient and novel carrier for the drug delivery system, due to slowing down the drug release and its non-cytotoxicity. Therefore, the toxicological studies about the coated NMOF-5 by silica were developed for the first time in the drug delivery systems.

Materials and Methods

All the reagents and solvents were purchased from Merck (Germany) and they were used without any further purification. Ultrasound irradiation was performed in an Elmasonic S ultrasonic cleaner with a frequency of 40 KHz and a normal power of 250 W. FT-IR spectra were recorded in KBr discs on an Alpha Bruker FT-IR spectrophotometer. The Brunauer–Emmett–Teller (BET) analyses were performed on the Belsorp-mini II. X-ray powder diffraction (XRD) patterns were recorded on an X'Pert MPD PRO powder X-ray diffractometer, using Cu Kα radiation. Thermogravimetric analyses were performed on a Perkin-Elmer TGA 7 from 25 ^oC to 700 ^oC at a heating rate of 10 °C.min^{-1} in the air. Field emission scanning electron microscopy (FE-SEM) was carried out using a MIRA3 TESCAN-XMU with the gold coating. UV/Vis spectra were recorded on a Beijing Rayleigh UV-1800 UV/Vis Spectrophotometer. The cell viability was determined using an ELISA plate reader (Biotek, Winooski, VT) at 490 nm with a reference wavelength of 630 nm.

Synthesis of the NMOF-5

The NMOF-5 nanoparticles were synthesized based on a previously reported procedure with a slight modification [22]. The supplementary details were presented in the supporting information file, according to the Scheme 1.

Drug loading

Incorporation of the drugs into the NMOF-5 was achieved through the following procedure: Two alcoholic solutions of acetaminophen (0.40 g in 16 mL) and ibuprofen (0.40 g in 12 mL) were prepared. The NMOF-5 (0.20 g) was added to each solution and the

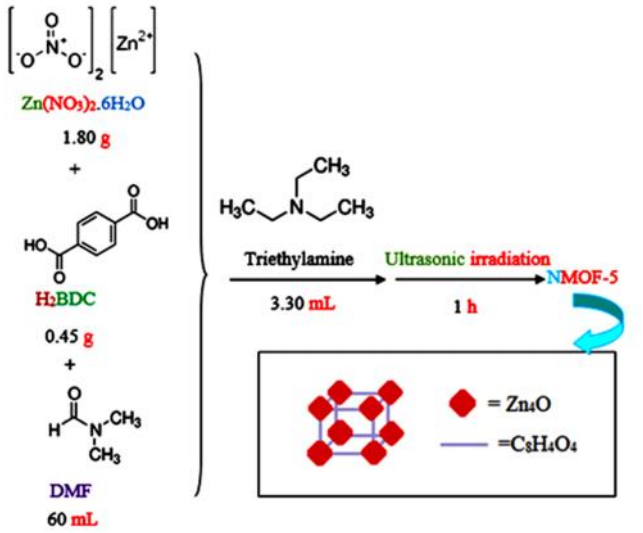

Scheme 1. A brief overview of the synthesis of NMOF-5

mixture was stirred for 24 h, while the measures were taken to prevent the solvent evaporation. Then, the solids were then separated by centrifugation at 4000 rpm for 5 min. They were washed with ethanol (3×5) to remove the excess drug, and they were also dried at 60 °C overnight to eliminate the traces of ethanol.

Silica coating on the drug-loaded NMOFs

The drug-loaded NMOF-5 samples were covered with a silica layer according to a previously reported study, with minor modifications [23]. The overall process was presented in details in the supporting information file, according to Scheme 2.

Preparation of the calibration curves

The Standard solutions of acetaminophen and ibuprofen with the concentrations of 5, 15, 25, 35 and 50 μg.mL^{-1} in PBS were prepared. The absorbance was plotted against the concentration at 242 nm for acetaminophen and at 222 nm for ibuprofen. The corresponding calibration curves were presented in the supplemantry files (Figures S1, S2).

The drug release tests

0.04 g of each drug loaded sample (NMOF-5@acetaminophen and NMOF-5@ibuprofen) and 0.04 g of each silica coated assembly (NMOF-5@acetaminophen@silica and NMOF-5@ibuprofen@silica) were dispersed under stirring in the simulated body fluid (PBS, pH 7.4, 5 mL) at 37 ^{o}C. At the predetermined time intervals, the dissolution medium was filtered and the supernatant was used to determine the drug concentration from the corresponding calibration curves by means of a UV/Vis spectrophotometer at 222 nm for ibuprofen and at 242

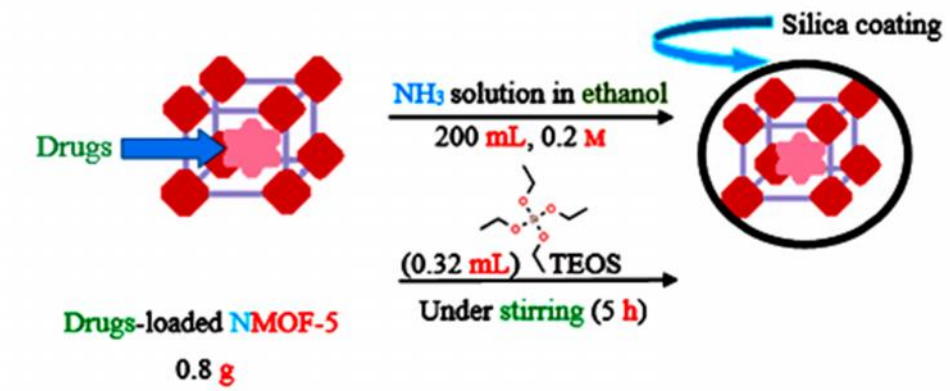

Scheme 2. A brief overview of silica coating on drugs-loaded NMOFs

nm for acetaminophen, respectively.

Cell seeding and MTT assay

The cell proliferation was measured using the MTT (Methylthiazolyldiphenyl-tetrazolium bromide) assay. The yellow MTT solution was reduced to the purple formazan in the living cells. In this research, NIH3T3 mouse embryonic fibroblast cells were used as the model cell line. (2×10^4) Cells/well were seeded in a well plate (48) in the complete media containing the DMEM medium (Bioidea, Glutamax high glucose), the heat-inactivated fetal bovine serum (Gibco, 15%) and the antibiotics (Bioidea, 100X penicillin/ streptomycin solution, 1%) for 24 h (5% CO_2, 37 °C, 95% humidity). Afterward, the medium was removed and the fresh media containing different concentration of NMOF-5 or NMOF-5@silica (20, 40, 60 and 80 $\mu g.mL^{-1}$) was added to the various wells of the plate. NIH3T3 cells with the same cell number of cells in the complete medium were used as the control. After 72 h of incubation, the old medium was replaced with the fresh MTT containing medium (0.5 $mg.mL^{-1}$ final concentration). The plate was incubated for 4 h and then the medium was removed. The resulted formazan crystals in each well were dissolved in the dimethylsulfoxide (DMSO, 50 µL). The plate was incubated with gentle shaking for 15 min at the room temperature. The absorbance was read by an enzyme-linked immunosorbent assay (ELISA) plate reader at 490 nm with a reference wavelength of 630 nm. The value of cell viability was calculated from Equation 1.

$$Cell\ Viability(\%) = \frac{(absorbance\ of\ sample)}{(absorbance\ of\ control)} \times 100$$

(Equation 1)

Statistical analysis

One way ANOVA was used to distinguish the differences between the control and the treatments and the result was significant ($P < 0.05$).

Results and Discussion

NMOF-5 was synthesized by addition of trimethylamine to a solution of $Zn(NO_3)_2 \cdot 6H_2O$ and 1,4-benzene dicarboxylic acid (H_2BDC) in DMF under the ultrasound irradiation [21]. Then, the alcoholic solutions of acetaminophen and ibuprofen were then treated with the NMOF-5 samples for 24 h to prepare NMOF-5@acetaminophen and NMOF-5@ibuprofen, respectively. To cover the drug-loaded samples with a layer of silica, ethanolic ammonia solution and TEOS were used [23]. The zeta potentials of NMOF-5, NMOF-5@ibuprofen, NMOF-5@acetaminophen, NMOF-5@silica, NMOF-5@ibuprofen@silica and NMOF-5@acetaminophen@silica were measured to be 0, +2.8, 0, -4.5, -4.5 and -4.5 mV, respectively. The zeta potential of NMOF-5@ibuprofen (+2.8 mV) confirmed that some ibuprofen was adsorbed into the surface of NMOF-5. In the FT-IR spectrum of NMOF-5 in supplemantry file (Figure S3 a) the following characteristic vibrations (cm^{-1}) were observed: 3544 (C-H aromatic stretching), 1570 (C=O stretching), 1400 and 1504 (aromatic C=C stretching) and 558 (Zn-O

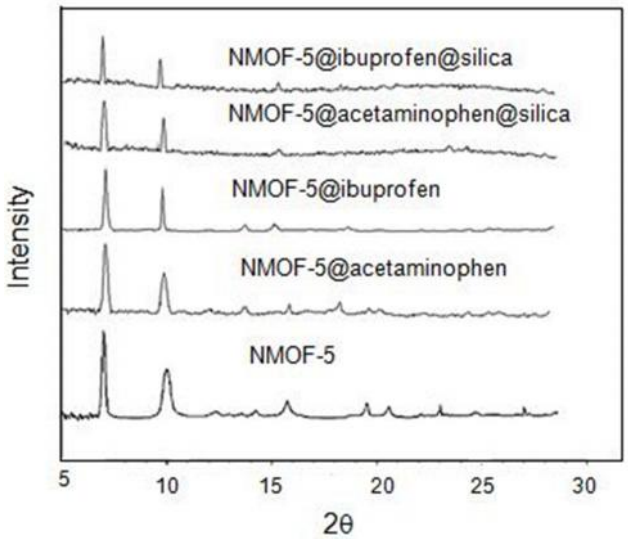

Figure 1. PXRD pattern of NMOF-5, NMOF-5@acetaminophen, NMOF-5@ibuprofen, NMOF-5@acetaminophen@silica, NMOF-5@ibuprofen@silica

band). The observed C-H aliphatic bands at 2924 and 2930 cm^{-1} in the FT-IR spectra of NMOF-5@acetaminophen and NMOF-5@ibuprofen in supplemantry file (Figures S3b, c) were related to the presence of acetaminophen and ibuprofen in the drug-loaded samples. After forming the silica coating, new bands were appeared at 1042, 1044 and 1019 cm^{-1}, which could be attributed to Si-O-Si symmetric stretching vibrations in the NMOF-5@acetaminophen@silica, NMOF-5@ibuprofen@silica and NMOF-5@silica in supplemantry file (Figure S4).

The powder X-ray diffraction pattern (PXRD) of NMOF-5 was shown in Figure 1, and it was in complete agreement with the previously reported pattern [22]. The PXRD patterns of the drug-loaded and the silica-coated samples were almost the same as NMOF-5, except that the intensity of the peaks of NMOF-5@acetaminophen@silica and NMOF-5@ibuprofen@silica were reduced due to the formation of an amorphous silica layer and the reduction of crystalline cubic structure of NMOF-5.

The thermogravimetric analyses (TGA) of the samples were shown in Figure 2. NMOF-5@acetaminophen (blue curve) showed a distinct 7% weight loss at the range of 300 to 400 ^{o}C, corresponding to the loss of acetaminophen. In comparison, a 19% weight loss, related to the removal of ibuprofen was observed at almost the same range for NMOF-5@ibuprofen (210 to 400 ^{o}C, Figure 2, red curve). Higher loading capacity of the NMOF-5 for the adsorption of ibuprofen may be related to the π-π interactions between the aromatic rings of ibuprofen and NMOF. In accordance with Figure 2 (green), 7% of the loss of acetaminophen was observed between 200 to

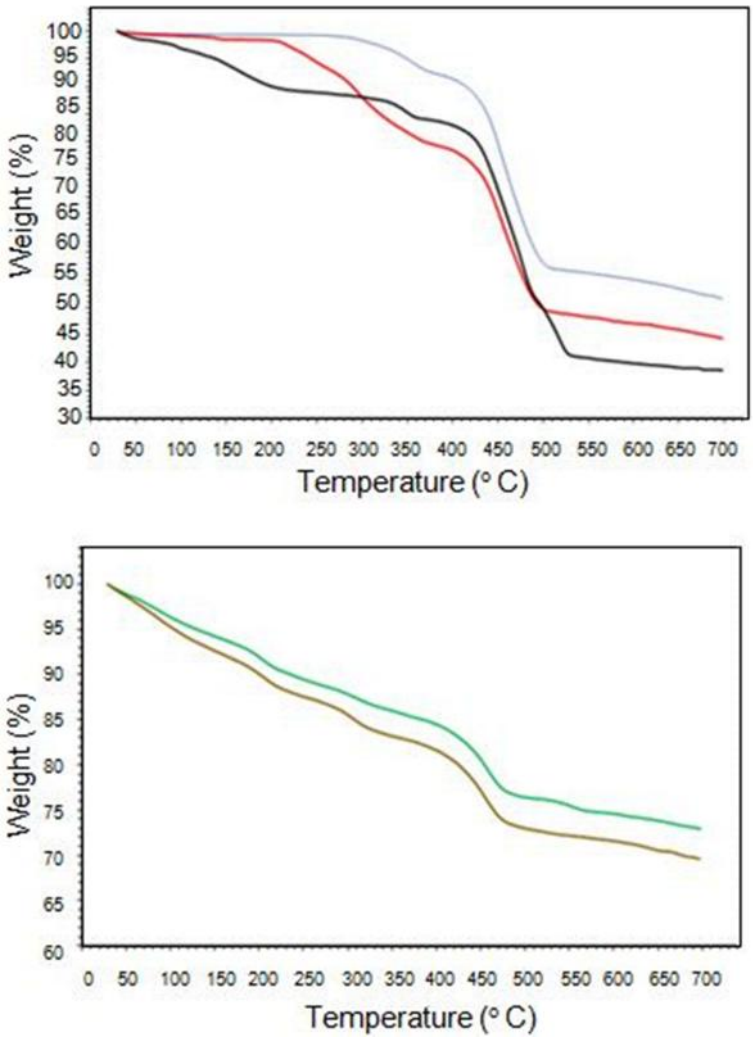

Figure 2. Thermogravimetric analysis of NMOF-5 (black), NMOF-5@acetaminophen (blue), NMOF-5@ibuprofen (red), NMOF-5@acetaminophen@silica (green), NMOF-5@ibuprofen@silica (brown).

390 °C. Ultimately, 7% of the loss of ibuprofen was observed between 220 to 370 °C which was shown in Figure 2 (brown). The thermal behaviour of NMOF-5@acetaminophen@silica (green curve) and NMOF-5@ibuprofen@silica (brown cure) was extremely similar, except that the NMOF-5@ibuprofen@silica had a higher weight loss in the range of 220 to 370 °C. It is also clear that the remaining weight of the last two cases was higher than the uncovered assemblies, which can be attributed to the presence of the thermally stable silica coating.

The Brunauer–Emmett–Teller (BET) analyses were used to determine the surface area and the pore size of the samples. The results for the specific surface area of NMOF-5, the ibuprofen and the acetaminophen loaded NMOF (Figure 3) showed that there was a decrease in the specific surface area from 1267 $m^2.g^{-1}$ (NMOF-5) to 47 $m^2.g^{-1}$ (ibuprofen loaded NMOF) and 32 $m^2.g^{-1}$ (acetaminophen loaded NMOF). Furthermore, these changes at the surface area were observed for NMOF-5@ibuprofen@silica (45 $m^2.g^{-1}$) and NMOF-5@acetaminophen@silica (11 $m^2.g^{-1}$) in supplemantry file (Figure S5). These results indicated that the drugs almost occupied the pores and channels of NMOFs. The Barret, Joyner and Halenda (BJH) model were used to identify the pore size distributions of the porous materials. The maximum distribution of the pore size of NMOF-5 was 3.8 nm (Figure 4). The BJH of NMOF-5@ibuprofen, NMOF-5@acetaminophen, NMOF-5@ibuprofen@silica and NMOF-

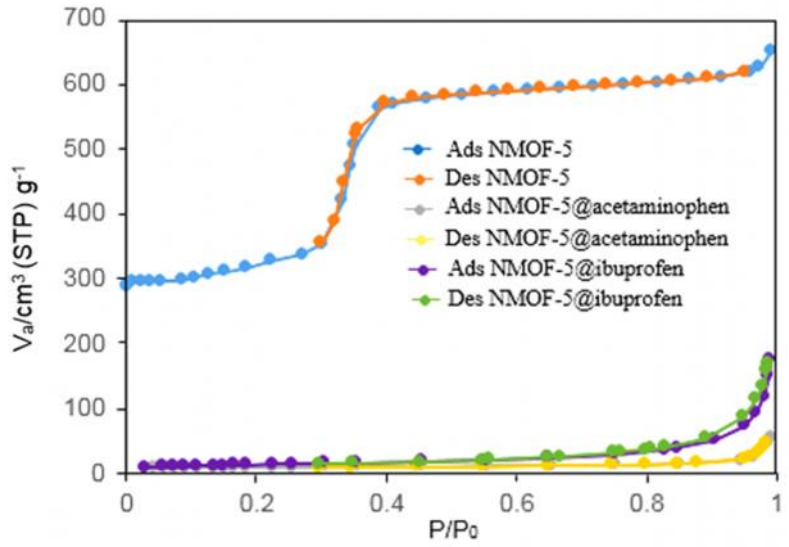

Figure 3. Nitrogen isotherm of NMOF-5, NMOF-5@acetaminophen, NMOF-5@ibuprofen

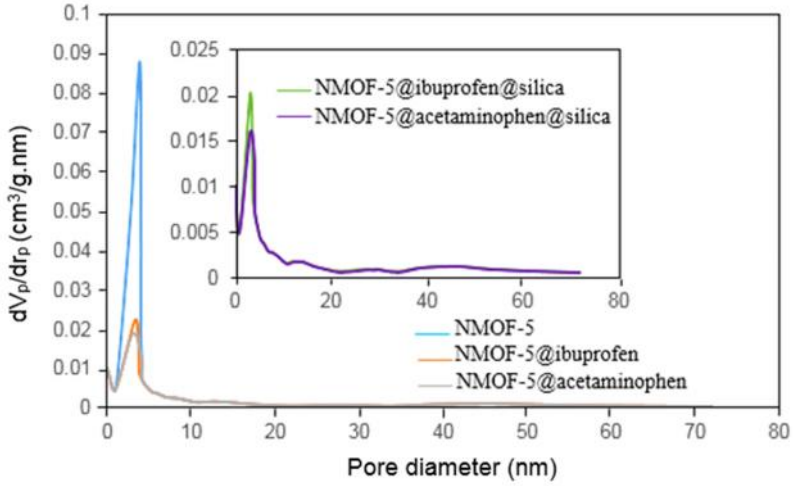

Figure 4. BJH pore size distribution of NMOF-5, NMOF-5@ibuprofen, NMOF-5@acetaminophen, NMOF-5@ibuprofen@silica, NMOF-5@acetaminophen@silica

5@acetaminophen@silica was shown in Figure 4. The decrease in the pore sizes of NMOF-5 in NMOF-5@ibuprofen (maximum distribution at 3.2 nm), NMOF-5@acetaminophen (maximum distribution at 3.0 nm), NMOF-5@ibuprofen@silica (maximum distribution at 3.1 nm) and NMOF-5@acetaminophen@silica (maximum distribution at 2.9 nm) suggested that the drugs were loaded in the pores of NMOF.

Ibuprofen and acetaminophen are widely used as the non-steroidal anti-inflammatory drugs (NSAID) to treat the pain and inflammatory diseases. These drugs, however, are associated with many side-effects which could be reduced by a sustained drug release. Figure 5 represents the release profile of acetaminophen and ibuprofen from the drug-loaded NMOF-5. A burst release was observed for both samples. The released content for NMOF-5@acetaminophen and NMOF-5@ibuprofen were 40 and 35% after 2 h, respectively. Complete release was achieved after 15 h for acetaminophen and 20 h for ibuprofen. While the results were still far from the ideal, we decided to protect the drug-loaded assemblies with a silica layer to overcome the burst release issue. The nature of the interactions between silica and NMOF-5 has been proposed to be the hydrogen bonding between MOF and silica.

Figure 6 demonstrates the release profile of acetaminophen and ibuprofen from the silica-coated assemblies. It is clear that the release profile was changed to a more appropriate form and the released amount was decreased after 2h to 5% for acetaminophen and 4% for ibuprofen, respectively. Complete drug release was achieved after 70 and 75 h for acetaminophen and ibuprofen, respectively. These results indicate a bright future for the drug-therapies. The main mechanism for the interaction of the drugs

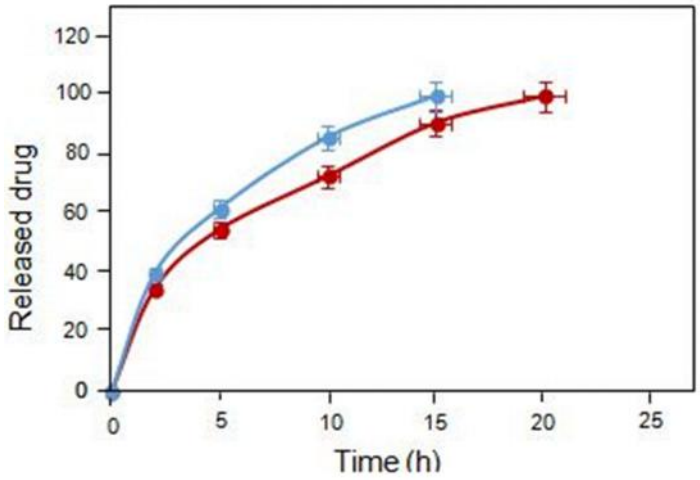

Figure 5. Percentage of ibuprofen release (red curve) and acetaminophen release (blue curve) from NMOF-5, in PBS PH=7.4 at 37 ^{o}C

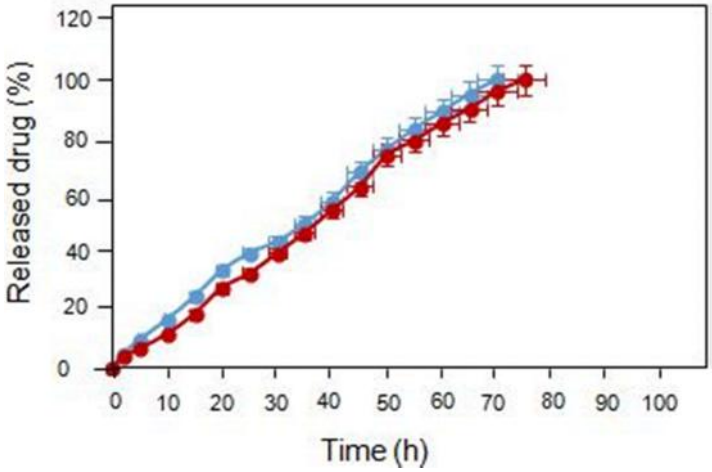

Figure 6. Ibuprofen (red curve) and acetaminophen (blue curve) delivery from NMOF-5@silica, in PBS PH=7.4 at 37 ^{o}C

with the composites suggested the π-π interactions between the aromatic rings of drugs and the organic part of the NMOF and van der waals forces between them [12].

To gain an insight into the morphology of the final products, the FE-SEM images were recorded. These images showed that NMOF-5 (Figure 7a), NMOF-5@acetaminophen (Figure 7b) and NMOF-5@ibuprofen (Figure 7c) adopt a cubic morphology with an average diameter of 35±10 nm. After coating with silica, however, a spherical morphology was observed for NMOF-5@acetaminophen@silica (Figure 7d) and NMOF-5@ibuprophen@silica (Figure 7e) with an average diameter of 50±15 nm.

In this study, the MTT assay was used in order to examine the toxic effects of the samples. The results of the MTT assay (Figure 8) showed that after 3 days of incubation with the concentration of 80 $\mu g.mL^{-1}$, the cell viability for NMOF-5, NMOF-5@silica, NMOF-5@ibuprofen, NMOF-5@acetaminophen, NMOF-5@acetaminophen@silica and NMOF-5@ibuprofen@silica was 6±0.7%, 103±1.4%, 4±0.7%, 3±0.0%, 74±4.9% and 78±3.5%, respectively. There was no cell toxic effect for NMOF-5@silica (103±1.4% viability), however, such effect strongly increased due to the concentration of 80 $\mu g.mL^{-1}$ of NMOF-5, NMOF-5@ibuprofen and NMOF-5@acetaminophen (6±0.7%, 4±0.7% and 3±0.0% viability, respectively). Therefore,

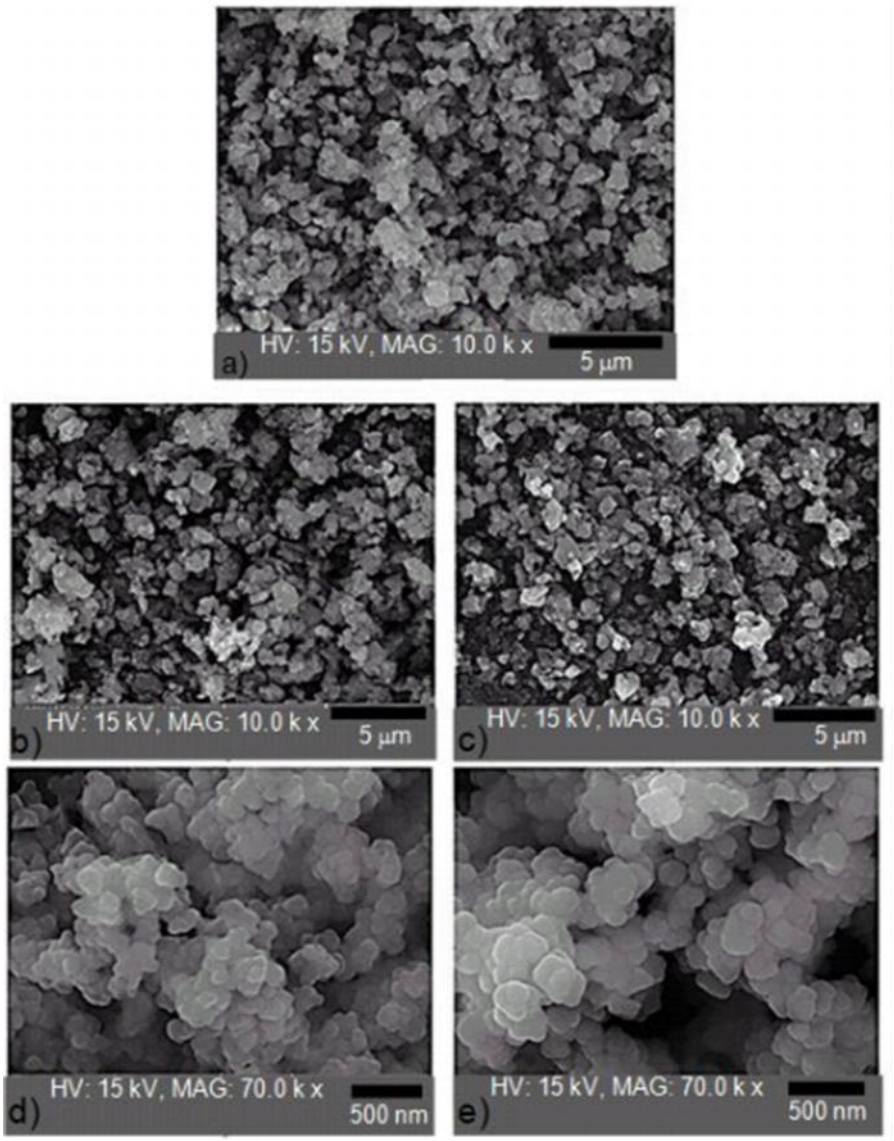

Figure 7. FE-SEM images of NMOF-5 (a), NMOF-5@acetaminophen (b), NMOF-5@ibuprofen (c), NMOF-5@acetaminophen@silica (d), NMOF-5@ibuprofen@silica (e).

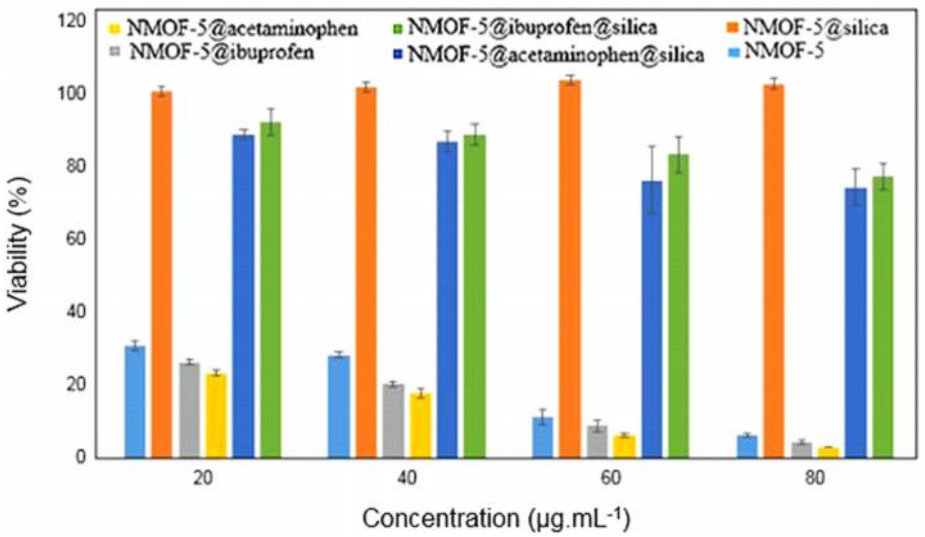

Figure 8. In vitro viability of NIH3T3 in the presence of NMOF-5, NMOF-5@silica, NNOF-5@ibuprofen, NMOF-5@acetaminophen, NMOF-5@ ibuprofen@silica and NMOF-5@acetaminophen@silica (n=3, $P < 0.05$)

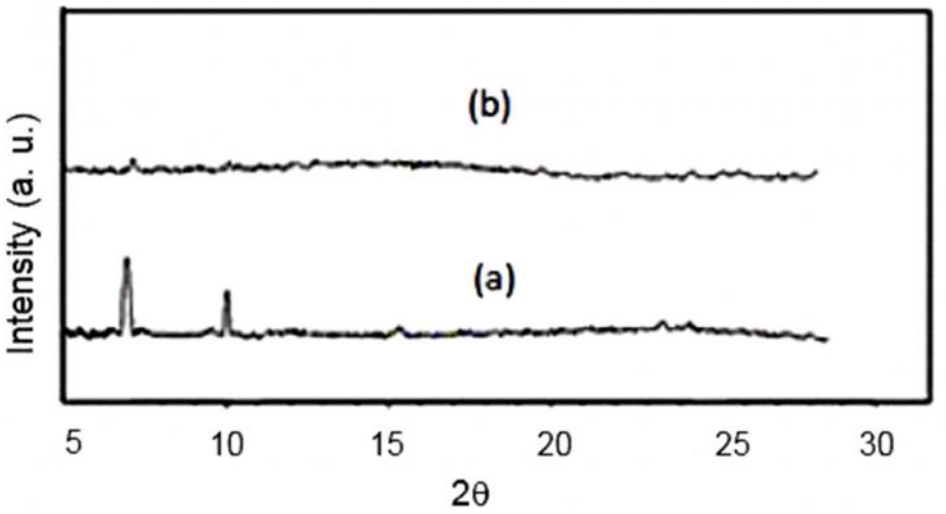

Figure 9. PXRD patterns for NMOF-5@silica (a) and NMOF-5 (b) after stirring for 75 and 20 h in PBS (PH=7.4) at 37 °C, respectively

the coating of NMOF-5 with silica reduced the toxic effect and improved the biocompatibility of NMOF-5. Because of the presence of acetaminophen and ibuprofen in the structure of this composite, the cell viability associated with concentration of 80 µg.mL^{-1} of NMOF-5@acetaminophen@silica and NMOF-5@ibuprofen@silica reached to 74±4.9% and 78±3.5%, respectively.

According to the results of the release profile of the drugs, it is clear that the surface modification of NMOF-5 with silica improved its stability and tuned its drug release rate. Moreover, the stability tests (Fig. 9) showed that NMOF-5@silica well tolerated the experimental conditions (stirring for 75 h in PBS at 37 °C), while NMOF-5 destroyed after stirring for 20 h in PBS at 37 °C. The biocompatibility and the sustained drug release were the unique features of our newly devised silica-coated NMOF-5@drug assemblies. It must be noted that the modification of NMOF-5 seems to be necessary in order to enhance its drug loading capacity.

Other similar works to improve the stability of MOF

by its coating for the drug delivery system include: The stability of MIL-100 (Fe) $\{Fe_3OH(H_2O)_2O(C_9H_3O_6)_2\}$ increased by its coating with β-cyclodextrin derivatives through the interaction between phosphate groups attached to β-cyclodextrin derivatives and iron(III) atoms [24]. Besides, variously modified cyclodextrin−MOFs materials with the enriched stability in an aqueous environment were effectively used [25-28]. The stability of MIL-101-NH_2 (Fe) particles in aqueous solution enhanced to some extent via the surface fluorine polymers coating [29]. In other studies, a copolymer Poly(N-isopropylacrylamide)-co-poly(N-acryloxysuccinimide)-co-poly(fluorescein O-methacrylate) and PEG (Polyethylene glycol) copolymers were used to improve the stability of Gd (III) NMOFs [18]. The other polymers, such as dextran, functionalized with biotin, chitosan grafted with alkyl side chains and poly(ethylene glycol) have been used to correct the surface of iron carboxylate NMOFs [18]. Polyvinylpyrrolidone and silica were used to cover Tb-based NMOFs to increase the stability of the NMOFs [18]. Likewise, a layer of silica was used to treat the surface of Mn-based and Gd-based NMOFs to increase their stability [18, 30]. The phosphorescent Zr-based MOFs were stabilized via a shell of silica and they were further improved with PEG and PEG–anisamide [23]. In another study, the stability in water of the MIL-101 (Fe) was remarkably enhanced because of the surface modification of NMOF with PEG [31]. Moreover, a lipid layer was also employed to modify NMOFs to enhance their stability [18]. Heparin was used to modify the surface of MIL-100 (Fe). The strong interactions between the iron metal sites of the MIL-100(Fe) and the sulfate groups of the heparin increased its stability [18]. In another similar study, a Na-exchanged ZMOF of the composition $[Na_{48}][In_{48}(HImDC)_{96}]$ (ImDC=4,5-imidazoledicarboxylate) was stabilized through the surface interactions with a series of large pore poly(hydroxyethylmethacrylate/2,3-dihydroxypropyl methacrylate/N-vinyl-2-pyrrolidone/ethylene glycol dimethacrylate) hydrogels [32]. Furthermore, The Fe-MIL-88B-NH_2 ($C_{48}Br_2Fe_6N_6O_{50.912}$) and Fe-MIL-100 improved their stability via chitosan coating [33, 34]. In, the other similar works, the UiO-66 ($C_{34.94}H_{17.47}O_{61.74}Zr_6$) enhanced its stability through coating by folic acid, biotin, PEG, poly-L-lactide, poly-N-isopropyl acrylamide and heparin [35, 36]. Also, the La-MOF was stabilized by graphene oxide and PEG, subsequently [37]. The HKUST-1 $[Cu_3(BTC)_2(H_2O)_3]$ improved its stability via coating by 4-Methyl phenyl dicyclohexyl ethylene [38]. Moreover, the $CaCO_3$ layer was used to treat the surface of NMOF and increased its stability [39]. Ethanolamine (EA) functionalized poly (glycidyl methacrylate) (PGMA-EA) was attached to UiO-66-NH_2 $[Zr_6O_4(OH)_4(BDC\text{-}NH_2)_6]$ to improve its stability in the gene delivery [40]. Also, UiO-66 was coated with poly(glycidyl methacrylate) and this carrier exhibited the appreciable colloidal stabilities in the biological milieu [41, 42]. The ZIF-8 ($C_8H_{10}N_4Zn$) was coated with methoxy poly (ethylene glycol)-folate (PEG-FA), demonstrating that this coating can enhance the stability of MOF [43, 44]. Similarly, MIL-100(Fe) was coated with PEG which increased the stability of NMOF [45]. Furthermore, ZrO_2 was used to modify the surface of ZIF-8 which improved its stability [46]. Additionally, coating of glucose on the Gd-NMOFs improved their biocompatibility and stability [47]. ZIF-8 was coated with sodium alginate and enriched its stability [48]. Dextran was grafted with both PEG and alendronate moieties, which are iron complexing groups anchored to the surface of the MIL-100 (Fe), and this increased its stability [49]. D-α-Tocopherol was succinated (α-TOS) in zeolitic imidazolate framework-8 (ZIF-8) compounds (defined as α-TOS@ZIF-8) and later it was coated with a hyaluronic acid (HA) shell to form the HA/α-TOS@ZIF-8 nanoplatform. This material improved the stability of ZIF-8 [50].

Therefore, the stability of NMOF in the drug delivery is a crucial challenge that requires more and more investigation about it.

Conclusions

It could be concluded that we devised a new platform for the sustained release of acetaminophen and ibuprofen, based on the NMOF-5 metal organic framework. The drug-loaded NMOFs were treated with a silica coating to overcome the burst release issue and the results were satisfying. It was found that NMOF-5@ibuprofen@silica and NMOF-5@acetaminophen@silica were able to deliver their complete drug content with a constant rate within 70 and 75 h, respectively. The silica coating also granted another important advantage. It was found that in vitro viability of NIH3T3 cells was significantly increased at the presence of NMOF-5@silica, NMOF-5@acetaminophen@silica and NMOF-5@ibuprofen@silica.

References

1. Yu S., Li S., Liu Y., Cui S. and Shen X., High-Performance Microporous Polymer Membranes Prepared by Interfacial Polymerization for Gas Separation. *J. Membrane Sci.* **573**: 425-438 (2019).
2. Nitani M., Nakayama K., Maeda K., Omori M. and Uno M., Organic Temperature Sensors Based on Conductive

Polymers Patterned by a Selective-Wetting Method. *Org. Electron.* **71**: 164-168 (2019).

3. Rabiee N., Hajebi S., Bagherzadeh M., Ahmadi S., Rabiee M., Roghani-Mamaqani H., Tahriri M., Tayebi L. and Hamblin M. R. Stimulus-Responsive Polymeric Nanogels as Smart Drug Delivery Systems. *Acta Biomater.* **92**: 1-18 (2019).
4. Rigby C. R., Han H., Bhowmik P. K., Bahari M., Chang A., Harb J. N., Lewis R. S. and Watt G. D., Soluble Viologen Polymers as Carbohydrate Oxidation Catalysts for Alkaline Carbohydrate Fuel Cells. *J. Electroanal. Chem.* **823**: 416-421 (2018).
5. Tranchemontagne D. J., Mendoza-Cortés J. L., O'Keeffe M. and Yaghi O. M., Secondary Building Units, Nets and Bonding in the Chemistry of Metal–Organic Frameworks. *Chem. Soc. Rev.* **38:** 1257-1283 (2009).
6. Hall J. N. and Bollini P., Structure, Characterization, and Catalytic Properties of Open-Metal Sites in Metal Organic Frameworks. *React. Chem. Eng.* **4(2)**: 207-222 (2019).
7. Yang D. and Gates B. C., Catalysis by Metal Organic Frameworks: Perspective and Suggestions for Future Research. *A. C. S. Catal.* **9(3)**: 1779-1798 (2019).
8. Qiao Z., Cheetham A. K. and Jiang J., Identifying the Best Metal–Organic Frameworks and Unravelling Different Mechanisms for the Separation of Pentane Isomers. *Mol. Syst. Des. Eng.* **4**: 609-615 (2019).
9. Connolly B. M., Aragones-Anglada M., Gandara-Loe J., Danaf N. A., Lamb D. C., Mehta J. P., Vulpe D., Wuttke S., Silvestre-Albero J., Moghadam P. Z. and Wheatley A. E., Tuning Porosity in Macroscopic Monolithic Metal-Organic Frameworks for Exceptional Natural Gas Storage. *Nat. Commun.* **10(1)**: 2345-2355 (2019).
10. Zhu C., Perman J. A., Gerald R. E., Ma S. and Huang J. Chemical Detection Using a Metal–Organic Framework Single Crystal Coupled to an Optical Fiber. *A. C. S. Appl. Mater. Inter.* **11(4)**: 4393-4398 (2019).
11. Martins L., Macreadie L. K., Sensharma D., Vaesen S., Zhang X., Gough J. J., O'Doherty M., Zhu N. Y., Rüther M., O'Brien J. E. and Bradley A. L., Light-Harvesting, 3rd Generation RuII/CoII MOF with a Large, Tubular Channel Aperture. *Chem. Commun.* **55(34)**: 5013-5016 (2019).
12. Motakef-Kazemi N., Shojaosadati S. and Morsali A., In Situ Synthesis of a Drug-Loaded MOF at Room Temperature. *Micropor. Mesopor. Mat.* **186:** 73-79 (2014).
13. Nejadshafiee V., Naeimi H., Goliaei B., Bigdeli B., Sadighi A., Dehghani S., Lotfabadi A., Hosseini M., Nezamtaheri M.S., Amanlou M. and Sharifzadeh M., Magnetic Bio-Metal–Organic Framework Nanocomposites Decorated with Folic Acid Conjugated Chitosan as a Promising Biocompatible Targeted Theranostic System for Cancer Treatment. *Mater. Sci. Eng. C.* **99:** 805-815 (2019).
14. Cho K., Wang X., Nie S., Chen Z. G., Shin D. M., Therapeutic Nanoparticles for Drug Delivery in Cancer. *Clin. Cancer. Res.* **14:** 1310-1316 (2008).
15. Darabi E., Ebadi N., Mehrabi S., Shakoori A. and Noori Daloii M. R., An Enrichment Method of Cell-free Fetal DNA from Mothers in the 11th Week of Pregnancy; On The Way of Non-invasive Prenatal Diagnosis of Beta-thalassemia as a Single Gene Disorder. *J. Sci. I. R. I.* **29(4)**: 305-309 (2018).
16. France M. M., del Rio T., Travers H., Raftery E., Xu K., Langer R., Traverso G., Lennerz J. K. and Schoellhammer C. M., Ultra-Rapid Drug Delivery in the Oral Cavity Using Ultrasound. *J. Control. Release.* **304**: 1-6 (2019).
17. Wang L. V. and Hu S., Photoacoustic Tomography: In Vivo Imaging from Organelles to Organs. *Sci.* **335(6075)**: 1458-1462 (2012).
18. Cai W., Chu C. C., Liu G. and Wáng Y. X. J., Metal–Organic Framework-Based Nanomedicine Platforms for Drug Delivery and Molecular Imaging. *Small.* **11:** 4806-4822 (2015).
19. Silva I. M. P., Carvalho M. A., Oliveira C. S., Profirio D. M., Ferreira R. B., Corbi P. P. and Formiga A. L., Enhanced Performance of a Metal-Organic Framework Analogue to MIL-101 (Cr) Containing Amine Groups for Ibuprofen and Nimesulide Controlled Release. *Inorg. Chem. Commun.* **70:** 47-50 (2016).
20. Wu Y. N., Zhou M., Li S., Li Z., Li J., Wu B., Li G., Li F. and Guan X., Magnetic Metal–Organic Frameworks: γ-Fe_2O_3@MOFs via Confined In Situ Pyrolysis Method for Drug Delivery. *Small.* **10**: 2927-2936 (2014).
21. Taylor-Pashow K. M., Della Rocca J., Xie Z., Tran S. and Lin W., Postsynthetic Modifications of Iron-Carboxylate Nanoscale Metal− Organic Frameworks for Imaging and Drug Delivery. *J. Am. Chem. Soc.* **131**: 14261-14263 (2009).
22. Li H., Eddaoudi M., O'Keeffe M. and Yaghi O. M., Design and Synthesis of an Exceptionally Stable and Highly Porous Metal-Organic Framework. *Nature.* **402(6759)**: 276-279 (1999).
23. Liu D., Huxford R. C. and Lin W., Phosphorescent Nanoscale Coordination Polymers as Contrast Agents for Optical Imaging. *Angew. Chem. Int. Ed.* **50**: 3696-3700 (2011).
24. Aykaç A., Noiray M., Malanga M., Agostoni V., Casas-Solvas J. M., Fenyvesi É., Gref R. and Vargas-Berenguel A., A Non-Covalent "Click Chemistry" Strategy to Efficiently Coat Highly Porous MOF Nanoparticles with a Stable Polymeric Shell. *Biochim. Biophys. Acta.* **1861(6)**: 1606-1616 (2017).
25. Hartlieb K. J., Ferris D. P., Holcroft J. M., Kandela I., Stern C. L., Nassar M. S., Botros Y. Y. and Stoddart J. F., Encapsulation of Ibuprofen in CD-MOF and Related Bioavailability Studies. *Mol. Pharm.* **14(5)**: 1831-1839 (2017).
26. Li H., Hill M. R., Huang R., Doblin C., Lim S., Hill A. J., Babarao R. and Falcaro P., Facile Stabilization of Cyclodextrin Metal–Organic Frameworks Under Aqueous Conditions via the Incorporation of C60 in Their Matrices. *Chem. Commun.* **52(35)**: 5973-5976 (2016).
27. Agostoni V., Horcajada P., Noiray M., Malanga M., Aykaç A., Jicsinszky L., Vargas-Berenguel A., Semiramoth N., Daoud-Mahammed S., Nicolas V. and Martineau C., A "Green" Strategy to Construct Non-Covalent, Stable and Bioactive Coatings on Porous MOF Nanoparticles. *Sci. Rep-UK.* **5:** 7925-7931 (2015).
28. Golmohamadpour A., Bahramian B., Shafiee A. and Ma'mani L., Slow Released Delivery of Alendronate Using β-Cyclodextrine Modified Fe–MOF Encapsulated

Porous Hydroxyapatite. *J. Inorg. Organomet. P.* **28(5)**: 1991-2000 (2018).
29. Liu S., Zhai L., Li C., Li Y., Guo X., Zhao Y. and Wu C., Exploring and Exploiting Dynamic Noncovalent Chemistry for Effective Surface Modification of Nanoscale Metal–Organic Frameworks. *A. C. S. Appl. Mater. Inter.* **6(8):** 5404-5412 (2014).
30. Rieter W. J., Taylor K. M. and Lin W., Surface Modification and Functionalization of Nanoscale Metal-Organic Frameworks for Controlled Release and Luminescence Sensing. *J. Am. Chem. Soc.* **129(32)**: 9852-9853 (2007).
31. Wang X. G., Dong Z. Y., Cheng H., Wan S. S., Chen W. H., Zou M. Z., Huo J. W., Deng H. X. and Zhang X. Z., A Multifunctional Metal–Organic Framework Based Tumor Targeting Drug Delivery System for Cancer Therapy. *Nanoscale.* **7(38)**: 16061-16070 (2015).
32. Bradshaw D., Garai A. and Huo J., Metal–Organic Framework Growth at Functional Interfaces: Thin Films and Composites for Diverse Applications. *Chem. Soc. Rev.* **41(6)**: 2344-2381 (2012).
33. Sivakumar P., Priyatharshni S., Nagashanmugam K. B., Thanigaivelan A. and Kumar K., Chitosan Capped Nanoscale Fe-MIL-88B-NH_2 Metal-Organic Framework as Drug Carrier Material for the pH Responsive Delivery of Doxorubicin. *Mater. Res. Express.* **4(8)**: 085023-085032 (2017).
34. Hidalgo T., Giménez-Marqués M., Bellido E., Avila J., Asensio M. C., Salles F., Lozano M. V., Guillevic M., Simón-Vázquez R., González-Fernández A. and Serre C., Chitosan-Coated Mesoporous MIL-100 (Fe) Nanoparticles as Improved Bio-Compatible Oral Nanocarriers. *Sci. Rep-UK.* **7:** 43112 (2017).
35. Abánades Lázaro I., Haddad S., Rodrigo-Muñoz J. M., Orellana-Tavra C., del Pozo V., Fairen-Jimenez D. and Forgan R. S., Mechanistic Investigation into the Selective Anticancer Cytotoxicity and Immune System Response of Surface-Functionalized, Dichloroacetate-Loaded, UiO-66 Nanoparticles. *A. C. S. Appl. Mater. Inter.* **10(6)**: 5255-5268 (2018).
36. Lázaro I. A., Haddad S., Sacca S., Orellana-Tavra C., Fairen-Jimenez D. and Forgan R. S., Selective Surface PEGylation of UiO-66 Nanoparticles for Enhanced Stability, Cell Uptake, and pH-Responsive Drug Delivery. *Chem.* **2(4)**: 561-578 (2017).
37. Xu C., Zhang C., Wang Y., Li L., Li L. and Whittaker A. K., Controllable Synthesis of a Novel Magnetic Core–Shell Nanoparticle for Dual-Modal Imaging and pH-Responsive Drug Delivery. *Nanotechnology.* **28(49):** 495101-495111 (2017).
38. Zhang L. P., Mo C. E., Huang Y. P. and Liu Z. S., Preparation of Liquid Crystalline Molecularly Imprinted Polymer Coated Metal Organic Framework for Capecitabine Delivery. *Part. Part. Syst. Char.* **36(1)**: 1800355-1800364 (2019).
39. Wan X., Zhong H., Pan W., Li Y., Chen Y., Li N. and Tang B. Programmed Release of Dihydroartemisinin for Synergistic Cancer Therapy Using a $CaCO_3$ Mineralized Metal-Organic Framework. *Angew. Chem. Int. Edit.* **58(40)**: 14134-14139 (2019).
40. Dong S., Chen Q., Li W., Jiang Z., Ma J. and Gao H., A Dendritic Catiomer with an MOF Motif for the Construction of Safe and Efficient Gene Delivery Systems. *J. Mater. Chem. B.* **5(42)**: 8322-8329 (2017).
41. Sun P., Li Z., Wang J., Gao H., Yang X., Wu S., Liu D. and Chen Q. Transcellular Delivery of Messenger RNA Payloads by a Cationic Supramolecular MOF Platform. *Chem. Commun.* **54(80)**: 11304-11307 (2018).
42. Chen S., Chen Q., Dong S., Ma J., Yang Y. W., Chen L. and Gao H., Polymer Brush Decorated MOF Nanoparticles Loaded with AIEgen, Anticancer Drug, and Supramolecular Glue for Regulating and In Situ Observing DOX Release. *Macromol. Biosci.* **18(12)**: 1800317-1800322 (2018).
43. Zhang H., Jiang W., Liu R., Zhang J., Zhang D., Li Z. and Luan Y., Rational Design of Metal Organic Framework Nanocarrier-Based Codelivery System of Doxorubicin Hydrochloride/Verapamil Hydrochloride for Overcoming Multidrug Resistance with Efficient Targeted Cancer Therapy. *A. C. S. Appl. Mater. Inter.* **9(23)**: 19687-19697 (2017).
44. Shi Z., Chen X., Zhang L., Ding S., Wang X., Lei Q. and Fang W., FA-PEG Decorated MOF Nanoparticles as a Targeted Drug Delivery System for Controlled Release of an Autophagy Inhibitor. *Biomater. Sci-UK.* **6(10)**: 2582-2590 (2018).
45. Giménez-Marqués M., Bellido E., Berthelot T., Simón-Yarza T., Hidalgo T., Simón-Vázquez R., González-Fernández Á., Avila J., Asensio M. C., Gref R. and Couvreur P., GraftFast Surface Engineering to Improve MOF Nanoparticles Furtiveness. *Small.* **14(40)**: 1801900-1801910 (2018).
46. Su L., Wu Q., Tan L., Huang Z., Fu C., Ren X., Xia N., Chen Z., Ma X., Lan X. and Zhang Q., High Biocompatible ZIF-8 Coated by ZrO_2 for Chemo-Microwave Thermal Tumor Synergistic Therapy. *A. C. S. Appl. Mater. Inter.* **11(11)**: 10520-10531 (2019).
47. Zhang H., Shang Y., Li Y. H., Sun S. K. and Yin X. B., Smart Metal–Organic Framework-Based Nanoplatforms for Imaging-Guided Precise Chemotherapy. *A. C. S. Appl. Mater. Inter.* **11(2)**: 1886-1895 (2018).
48. Vahed T. A., Naimi-Jamal M. R. and Panahi L., Alginate-Coated ZIF-8 Metal-Organic Framework as a Green and Bioactive Platform for Controlled Drug Release. *J. Drug Deliv. Sci. Tec.* **49**: 570-576 (2019).
49. Cutrone G., Qiu J., Menendez-Miranda M., Casas-Solvas J. M., Aykaç A., Li X., Foulkes D., Moreira-Alvarez B., Encinar J. R., Ladavière C. and Desmaële D., Comb-Like Dextran Copolymers: A Versatile Strategy to Coat Highly Porous MOF Nanoparticles with a PEG Shell. *Carbohyd. Polym.* **223**: 115085-115096 (2019).
50. Sun Q., Bi H., Wang Z., Li C., Wang X., Xu J., Zhu H., Zhao R., He F., Gai S. and Yang P., Hyaluronic Acid-Targeted and pH-Responsive Drug Delivery System Based on Metal-Organic Frameworks for Efficient Antitumor Therapy. *Biomaterials.* **223**: 119473-119483 (2019).